Redox Biology 15 (2018) 109–114

Contents lists available at ScienceDirect

Redox Biology

journal homepage: www.elsevier.com/locate/redox

Short communication

Cytochrome b_5 reductase is the component from neuronal synaptic plasma membrane vesicles that generates superoxide anion upon stimulation by cytochrome *c*

Alejandro K. Samhan-Arias[a,*], Sofia Fortalezas[b], Cristina M. Cordas[a], Isabel Moura[a], José J.G. Moura[a], Carlos Gutierrez-Merino[b,*]

[a] UCIBIO, REQUIMTE, Departamento de Quimica, Faculdade de Ciências e Tecnologia, Universidade Nova de Lisboa, 2829-516 Caparica, Portugal
[b] Department of Biochemistry and Molecular Biology, Faculty of Sciences, and Institute of Molecular Pathology Biomarkers, University of Extremadura, 06006 Badajoz, Spain

ARTICLE INFO

Abbreviations:
Cb_5R, Cytochrome b_5 reductase
DTPA, Diethylenetriaminepentaacetic acid
DHE, Dihydroethidium
E^+, Ethidium
FAD, Flavin adenine dinucleotide
NADH, Reduced nicotinamide adenine dinucleotide
NBT, Nitroblue tetrazolium nitroblue tetrazolium
SPMV, Synaptic plasma membrane vesicles
TB, Terrific Broth terrific Broth
SOD, Superoxide dismutase
XA, Xanthine xanthine
XO, Xanthine oxidase

Keywords:
Cytochrome *c*
Superoxide anion
NADH oxidase
Cytochrome b_5 reductase
Neurons

ABSTRACT

In this work, we measured the effect of cytochrome *c* on the NADH-dependent superoxide anion production by synaptic plasma membrane vesicles from rat brain. In these membranes, the cytochrome *c* stimulated NADH-dependent superoxide anion production was inhibited by antibodies against cytochrome b_5 reductase linking the production to this enzyme. Measurement of the superoxide anion radical generated by purified recombinant soluble and membrane cytochrome b_5 reductase corroborates the production of the radical by different enzyme isoforms. In the presence of cytochrome *c*, a burst of superoxide anion as well as the reduction of cytochrome *c* by cytochrome b_5 reductase was measured. Complex formation between both proteins suggests that cytochrome b_5 reductase is one of the major partners of cytochrome *c* upon its release from mitochondria to the cytosol during apoptosis. Superoxide anion production and cytochrome *c* reduction are the consequences of the stimulated NADH consumption by cytochrome b_5 reductase upon complex formation with cytochrome *c* and suggest a major role of this enzyme as an anti-apoptotic protein during cell death.

1. Introduction

The plasma membrane NADH oxidase activity of cerebellar granule neurons represents a disguisable activity producing superoxide anion ($O_2^{\cdot-}$) as a collateral product of NADH consumption [1–4]. The plasma membrane constituents associated to this activity are not well defined although it is known that cytochrome b_5 reductase (Cb_5R) is one of its major components present at the plasma membrane of rat cerebellar granule neurons in culture and of synaptic plasma membrane vesicles (SPMV) from rat brain [1]. This protein increases its association to lipids rafts in apoptosis [2]. In addition, 1–3 h after apoptosis induction an increment of $O_2^{\cdot-}$ has been detected at the peripheral neuronal plasma membrane [2]. This event correlates with the observed times for cytochrome *c* (Cyt *c*) release from mitochondria to the cytosol, as soon as 1 h after apoptosis induction, although the maximum peak for its release was found at 3 h [2].

In this work, we described the function of Cyt *c* as activator of the $O_2^{\cdot-}$ production by Cb_5R, as a component of SPMV, and results were experimentally confirmed with two isoforms of human Cb_5R. Due to the important role of Cyt *c* redox state in apoptosis and its reduction by Cb_5R, we propose a function of Cb_5R, as one the main defensive components during apoptosis after Cyt *c* release from mitochondria to the cytosol.

* Corresponding authors.
E-mail addresses: alejandro.samhan@fct.unl.pt (A.K. Samhan-Arias), carlosgm@unex.es (C. Gutierrez-Merino).

https://doi.org/10.1016/j.redox.2017.11.021
Received 19 October 2017; Received in revised form 23 November 2017; Accepted 24 November 2017
Available online 27 November 2017

2. Materials and methods

2.1. SPMV preparation

Rat brain SPMV were prepared using a standard procedure as described in [1,3].

2.2. Human Cb_5R isoforms cloning

Cloning of Cb_5R isoforms was performed as indicated in [5] using commercially available construct for soluble and primers described in Supplementary material.

2.3. Purification of recombinant human Cb_5R isoforms

Clones of Cb_5R isoforms were overexpressed in DE3 competent cells (Rosetta Gammi 2, Novagen) and the recombinant protein purified as indicated in [5].

2.4. NADH oxidase activity

NADH oxidase was measured at 37 °C as in [1,3,4,6,7].

2.5. O_2 consumption

O_2 consumption was measured using an Oxygraph Plus DW1 (Hansatech instruments) electrode in the same buffer described above, in presence of NADH (50 μM) and purified human recombinant Cb_5R isoforms at 37 °C.

2.6. $O_2^{\cdot-}$ measurement with NBT

$O_2^{\cdot-}$ production by Cb_5R was calculated measuring the reduction of NBT in the same buffer described above at pH 7.0, with NBT 200 μM and SOD 1 U/mL at 560 nm at 37 °C using a ε of 27.8 mM^{-1} cm^{-1} [8,9].

2.7. Cyclic voltammetry

Qualitative measurement of the $O_2^{\cdot-}$ generated by Cb_5R was performed by cyclic voltammetry with a pyrolytic graphite electrode using the thin layer technique (membrane cut off 3.5 kDa) [5]. Cb_5R (0.6 mM) or albumins (0.6 mM) as a control were loaded onto the electrode. The set up was completed with a silver/silver chloride (Ag/AgCl) reference electrode and a platinum counter electrode to complete the three electrodes cell configuration.

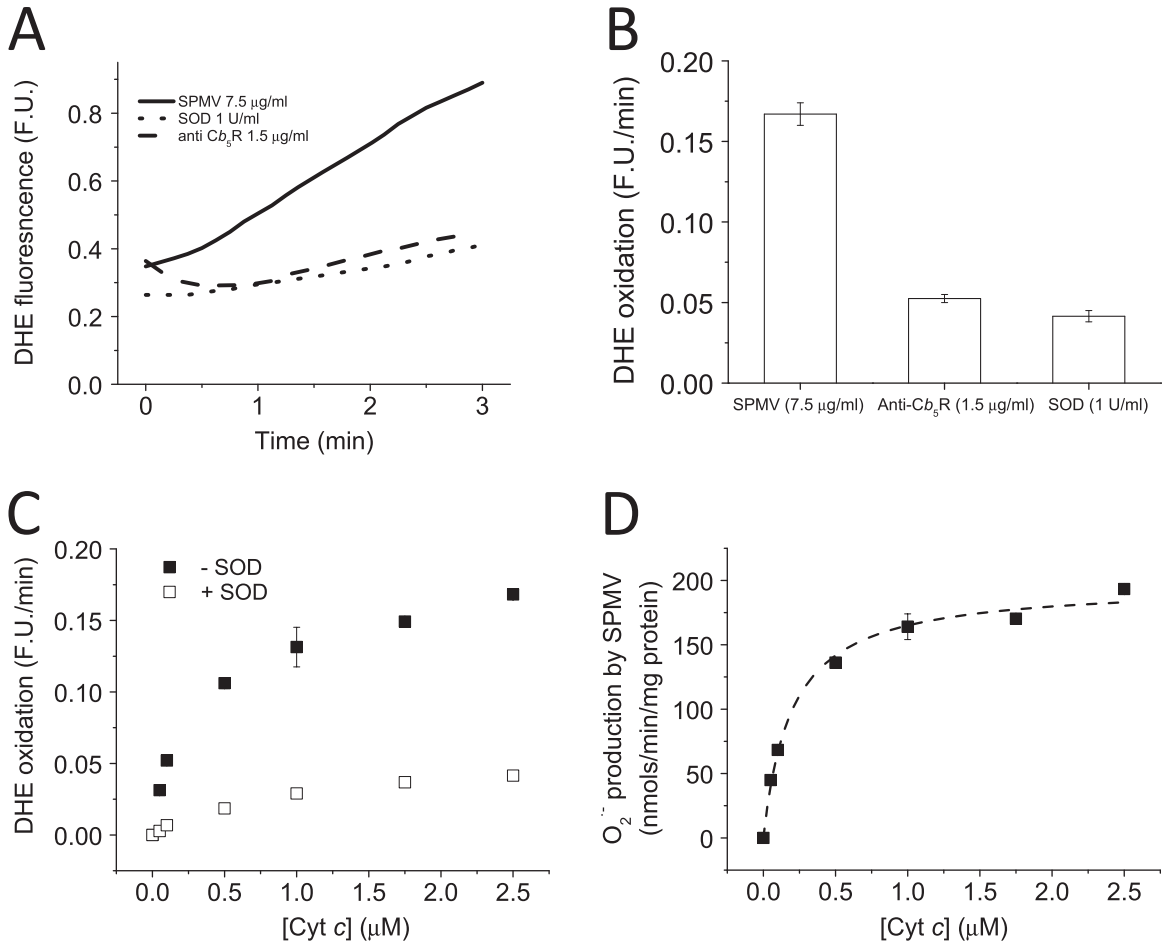

Fig. 1. Cyt *c* stimulated NADH-dependent $O_2^{\cdot-}$ production by SPMV. Panel A : Kinetics of the NADH dependent DHE oxidation by SPMV measured by fluorescence in the absence and presence of SOD (1 U/mL) and anti- Cb_5R antibody (1.5 μg/mL). DHE oxidation was measured at 37 °C in potassium phosphate 20 mM plus DTPA 0.1 mM (pH 7.0), using a Perkin Elmer spectrofluorimeter with 470 nm and 605 nm excitation and emission wavelengths, respectively, and 10 nm excitation and emission slits. Representative traces of DHE oxidation by SPMV (7.5 μg/mL) in the presence of NADH (50 μM), oxidized Cyt *c* (Fe^{3+}) (2.5 μM) and DHE (2 μM),in the presence of 1.5 μg/mL anti-Cb_5R (dashed line) or 1 U/mL SOD (dotted line) are shown. **Panel B**: Quantification of the inhibition induced by anti-Cb_5R (1.5 μg/mL) and SOD (1 U/mL) on the DHE oxidation rate by SPMV (7.5 μg/mL) in the presence of NADH (50 μM) and oxidized Cyt *c* (Fe^{3+}) (2.5 μM). **Panel C**: Dependence of the NADH-dependent DHE oxidation rate by SPMV (7.5 μg/mL) upon Cyt *c* concentration in the absence (filled squares) or in the presence of SOD (1 U/mL) (open squares). **Panel D**: NADH dependent $O_2^{\cdot-}$ production by SPMV (7.5 μg/mL) dependence upon Cyt *c* concentration, measured with DHE. All the results shown in this Figure are the average (± standard errors) of experiments done by triplicate.

2.8. $O_2^{\cdot-}$ measurement with DHE

$O_2^{\cdot-}$ formation was measured by fluorescence using dihydroethidium (DHE) [10]. Measurements were performed at 37 °C in buffer (pH 7.0) potassium phosphate 20 mM, DTPA 0.1 mM, and DHE 2 μM and Cyt *c* at the concentration indicated in each experiment, using a quartz cuvette. Fluorescence of DHE was measured with 470 nm and 605 nm excitation and emission wavelengths, respectively, and slits of 10 nm. Xanthine/Xanthine oxidase (XA/XO) was used to calibrate the signal.

2.9. Cb_5R:Cyt c complex formation

Complex formation was measured at 37 °C as indicated in [5].

3. Results

3.1. $O_2^{\cdot-}$ production by SPMV NADH oxidase activity is stimulated by Cyt c

We measured the effect of oxidized Cyt *c* (Fe^{3+}) on the NADH-dependent $O_2^{\cdot-}$ production by SPMV with DHE. Addition of Cyt *c* (2.5 μM) to the assay produced more than 3-fold increase in the oxidation of DHE, in the presence of SPMV (7.5 μg/mL) and NADH (50 μM) (Fig. 1A, continuous line and B). In addition, SOD added to the assay blocked the Cyt *c* stimulated DHE oxidation rate by SPMV (Fig. 1A, dotted line and B), pointing out that the increased DHE oxidation rate was due to production of $O_2^{\cdot-}$, as expected for a $O_2^{\cdot-}$ responsive dye [11]. The effect of a specific antibody against Cb_5R (ProteinTech, Cat #4668234) in this assay was also tested (Fig. 1A, dashed line and B). The $O_2^{\cdot-}$ production by SPMV was almost completely inhibited, i.e. ≥ 90 % inhibition, in the presence of the specific antibody against Cb_5R. We measured the DHE oxidation rate dependence upon Cyt *c* (Fe^{3+}) concentration, in the absence (filled squares) and presence of SOD (1 U/mL) (open squares) (Fig. 1C). Addition of increasing concentrations of Cyt *c* to the assay produced a Cyt *c* dependent increase of the DHE oxidation rate. Calibration curves for $O_2^{\cdot-}$ production vs. DHE oxidation were generated using increasing XO concentrations (Supplementary Fig. S1). Thereafter, we calculated that Cyt *c* was stimulating the NADH-dependent $O_2^{\cdot-}$ production by SPMV almost 20-fold, reaching a maximum value of 192 ± 41 nmoles/min/mg protein, in comparison to the activity measured in absence of Cyt *c* (10 nmoles/min/mg protein) (Fig. 1D). The NADH dependent $O_2^{\cdot-}$ production dependence upon Cyt *c* concentration yielded a K_m for Cyt *c* stimulation of 0.2 ± 0.03 μM.

3.2. Measurement of the $O_2^{\cdot-}$ production by recombinant Cb_5R isoforms

3.2.1. $O_2^{\cdot-}$ production by Cb_5R

The oxidation of NADH by soluble and membrane purified Cb_5R isoforms (Fig. 2 and Supp. Fig. S2A, respectively) was linearly dependent upon protein concentration (Fig. 2D). The calculated NADH oxidase activity of soluble and membrane Cb_5R was 0.27 ± 0.02 and 0.15 ± 0.02 μmoles/min/mg of protein, respectively. Under the same experimental conditions the kinetics of O_2 consumption, in the presence

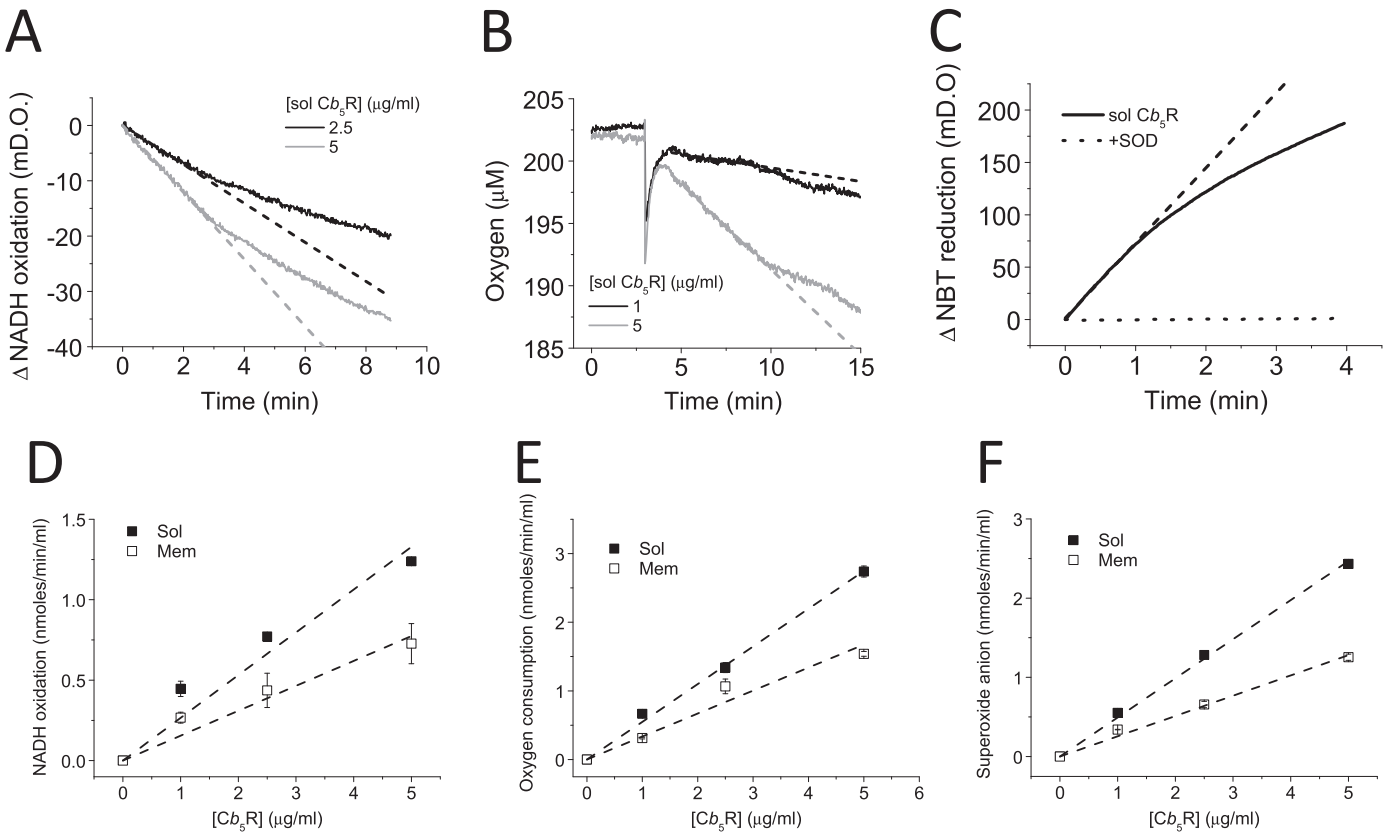

Fig. 2. Correlation between NADH oxidation, O_2 consumption and superoxide anion production by soluble Cb_5R. Panel A : Representative traces of the NADH oxidation by soluble Cb_5R (2.5 and 5 μg/mL) are shown. NADH oxidase activity was measured from absorbance decay at 340 nm at 37 °C, in the following assay medium (pH 7.0): potassium phosphate 20 mM, DTPA 0.1 mM, NADH 100 μM in presence of soluble Cb_5R 2.5 (black line) and 5 μg/mL (grey line). Dotted lines indicate the slopes used to calculate the activity. **Panel B**: Oxygen consumption kinetics for soluble Cb_5R 1 μg/mL (black line) 5 μg/mL (grey line). The reaction was started by addition of Cb_5R at the time marked by a large drop of trace signals. O_2 consumption was measured in presence of soluble Cb_5R using a Oxygraph Plus DW1 (Hansatech Instruments) electrode, filled with 2 mL of the assay medium indicated in the Panel A. Dotted lines indicate the slopes used to calculate the activity. **Panel C:** $O_2^{\cdot-}$ production by soluble Cb_5R was measured with NBT. Representative traces for the kinetics of NBT reduction by soluble Cb_5R isoform, and sensitivity to SOD is shown. NBT reduction was measured at 37 °C at 560 nm with soluble Cb_5R 2.5 μg/mL in absence (black line) or presence of SOD 1 U/mL (dotted line) in the assay medium indicated in the Panel A, supplemented with NBT 200 μM. The dotted line indicates the slope used to calculate the activity. **Panels D, E and F**: Dependence upon Cb_5R concentration for soluble (filled squares) and membrane (open squares) Cb_5R, respectively, of NADH oxidation, oxygen consumption and superoxide production. All the results shown in this Figure are the average (± standard errors) of triplicate experiments.

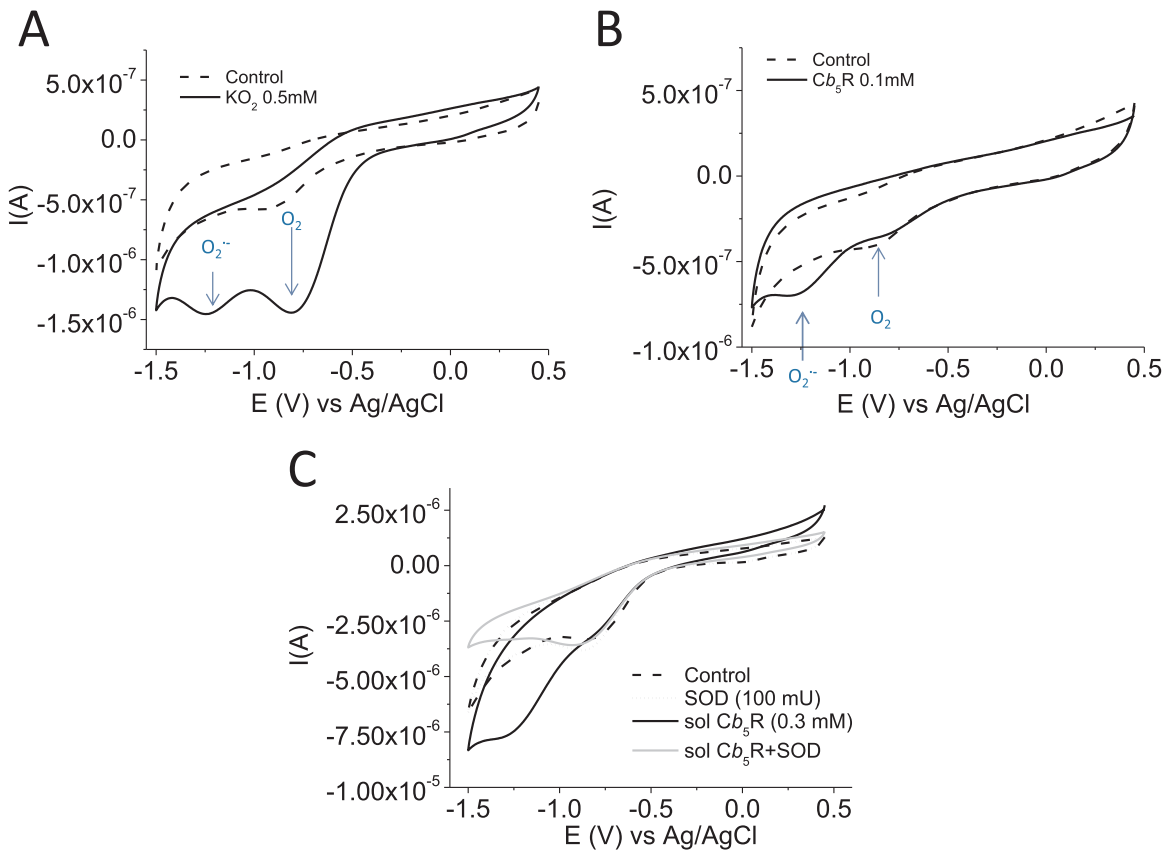

Fig. 3. Qualitative measurement of the $O_2^{\cdot-}$ production by soluble Cb_5R using cyclic voltammetry. Representative voltammograms of KO_2 added to the buffer (continuous line) vs its absence (dashed line) measured using thin layer technique with a membrane (cut off 3.5 kDa) with control/albumin is shown in **panel A**. Electrolyte: 20 mM Phosphate buffer / 0.1 M KCl pH 7.0 in presence of atmospheric O_2. Scan rate: 5 mV/s. Proteins concentration: 0.1 mM. Layer thickness approx. 18 mm. **Panel B**: Typical voltammograms of Cb_5R (continuous line) vs. the control/albumin (dashed line) using thin layer technique with a membrane (Cutoff 3.5 kDa), recorded under the same conditions of Panel **A. Panel C**: Effect of SOD addition over the $O_2^{\cdot-}$ production by soluble Cb_5R. Representative voltammograms in the presence of SOD 0.1 U/mL (dotted line) vs. control/albumin (dashed line) are compared to the ones obtained for soluble Cb_5R (0.1 mM) (black line) vs. soluble Cb_5R (0.1 mM) in presence of SOD (0.1 U/mL) (grey line). Conditions were the same used in previous panels. All the results shown in this Figure are representative of triplicate experiments.

of NADH, by the soluble and membrane isoform of Cb_5R (Fig. 2B and Supp. Fig. S2B, respectively) yielded an O_2 consumption rate of 0.54 ± 0.02 and 0.33 ± 0.04 μmoles/min /mg protein for soluble and membrane Cb_5R respectively, calculated from the linear regression plot obtained with increasing enzyme concentrations (Fig. 2E). $O_2^{\cdot-}$ was measured from the SOD-inhibited NBT reduction (Fig. 2C and Supp. Fig. S2C), yielding a rate of $O_2^{\cdot-}$ production by soluble and membrane Cb_5R of 0.49 ± 0.02 and 0.26 ± 0.02 μmoles/min /mg of protein, respectively, from the slope of the linear dependence with Cb_5R concentration (Fig. 2F). Thus, these results yielded a stoichiometry of ≈ 2 molecules of $O_2^{\cdot-}$ generated per molecule of oxidized NADH and a good coherence for the results obtained with these three methods.

Cyclic voltammetry can be used for experimental assessment of $O_2^{\cdot-}$ production [12–16]. On these grounds, we have used this technique to further confirm $O_2^{\cdot-}$ production by Cb_5R. The measurement of this radical was first calibrated using KO_2 as a model compound. Two peaks appeared dependent on two generated components over the control: one at 1.25 V and another one at 0.8 V that were assigned to $O_2^{\cdot-}$ and O_2, respectively (Fig. 3A). In presence of Cb_5R (panel B), a signal similar to the observed for $O_2^{\cdot-}$ (using KO_2) appears, at the same potential, and the O_2 signal decreased correlating with O_2 consumption by the enzyme to generate $O_2^{\cdot-}$. In presence of SOD, the $O_2^{\cdot-}$ measured signal generated by Cb_5R was equal to control (panel 3C).

3.2.2. *Cyt c stimulated $O_2^{\cdot-}$ production by Cb_5R*

The NADH-dependent DHE oxidation rate by purified Cb_5R was almost completely inhibited by the presence of SOD in the assay medium (Fig. 4A). The Cyt *c* stimulated $O_2^{\cdot-}$ production by Cb_5R (1 mg/mL) was also reliably monitored with DHE (Fig. 4B) by the dependence upon Cyt *c* (Fe^{3+}) of the initial DHE oxidation rate. As Cyt *c* reduction has also been used as an indicator to monitor $O_2^{\cdot-}$ production [17,18], we have experimentally assessed whether the SOD inhibited reduction of Cyt *c* can reliably monitor the NADH-dependent $O_2^{\cdot-}$ production by purified Cb_5R. The kinetics of Cyt *c* reduction by Cb_5R in absence (continuous line) and presence of SOD (dashed line) is shown in Fig. 4C. These results showed that SOD (1 U/mL) inhibits by 40-45 % the reduction of Cyt *c* upon incubation in the assay for 45 min, and about the same reduction of the initial rate of reduction up to 5–10 min. This result is in contrast with the almost complete inhibition by SOD (1 U/ml)of the Cyt *c* stimulated DHE oxidation by Cb_5R, and pointed out that the reduction of Cyt *c* was the sum of two different kinetic processes: (1) direct reduction by Cb_5R which can use Cyt *c* as a final electron acceptor, and (2) reduction of Cyt *c* by the $O_2^{\cdot-}$ released by Cb_5R.

Therefore, for a proper kinetic analysis of $O_2^{\cdot-}$ production we measured the dependence of the DHE oxidation rate upon Cyt *c* and DHE concentration, using a fixed Cb_5R concentration and a fixed concentration of one of the twosubstrates for $O_2^{\cdot-}$ detection, as indicated in the Supp. material. The data were fit to a two substrate Michaelis-Menten kinetic model (Fig. 4 D and E). To calculate the $O_2^{\cdot-}$ production, we calibrated the oxidation of DHE by XA/XO (Supp. Fig. 1B and C). From titration results with different Cyt *c* concentrations and fixed DHE (2 μM) and Cb_5R (1 μg/mL) concentration, we calculated a k_{cat} for $O_2^{\cdot-}$ production by soluble and membrane Cb_5R of 1.37 ± 0.02 and 1.17 ± 0.02 s^{-1}, with a K_m for Cyt *c* of 0.29 ± 0.01 and 0.42 ± 0.02 μM, respectively (Fig. 4D). From titration with different DHE concentrations and fixed Cyt *c* (2.5 μM) and Cb_5R (1 μg/mL)

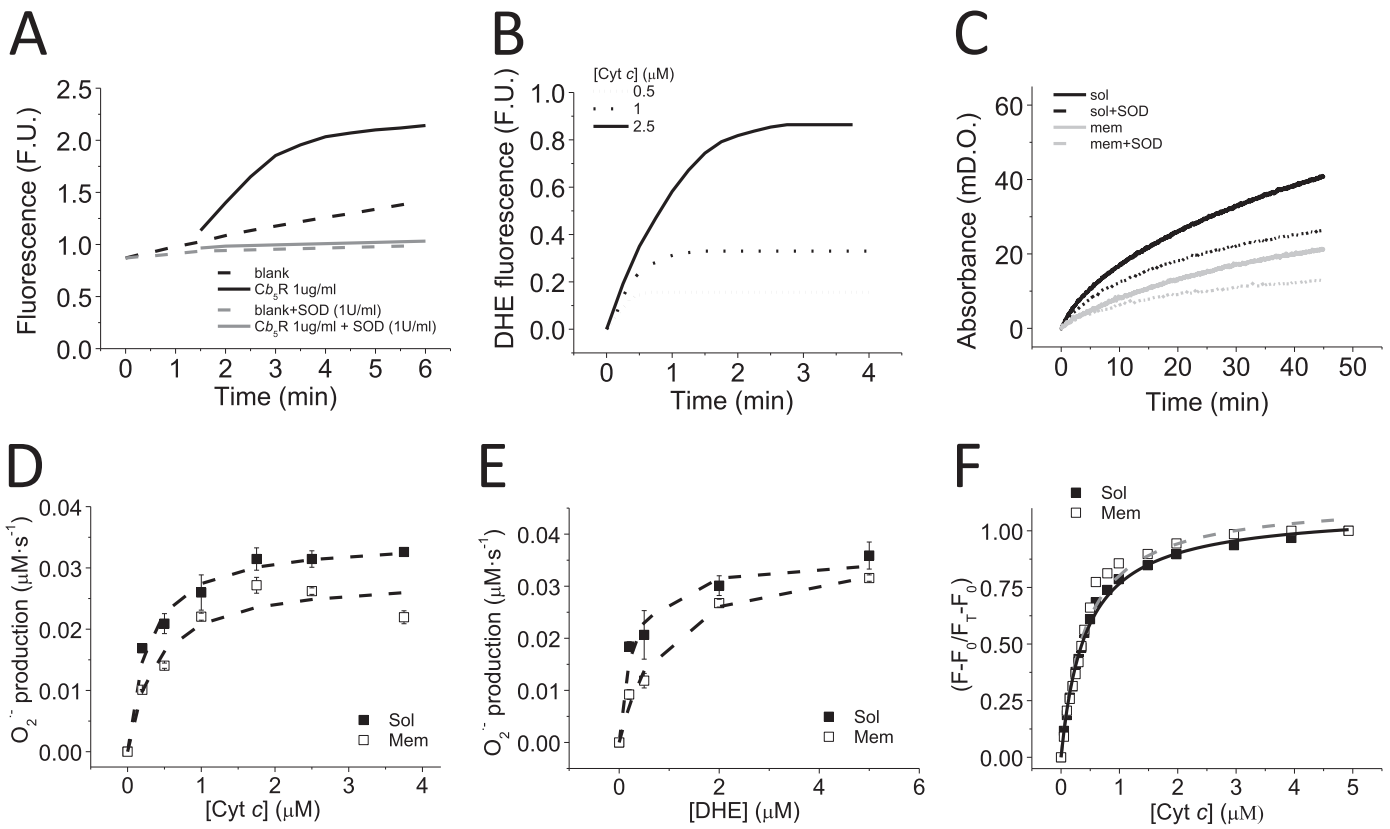

Fig. 4. DHE oxidation by C*b*$_5$R is almost completely inhibited by SOD and Cyt *c* stimulated $O_2^{\cdot-}$ production by C*b*$_5$R. Panel A: Kinetics of DHE oxidation by soluble C*b*$_5$R (continuous line) vs. blank (dashed line) in absence (black line) and presence of 1 U/mL SOD (grey line). DHE oxidation was measured at 37 °C in the following assay medium (pH 7.0): potassium phosphate 20 mM, DTPA 0.1 mM, NADH 50 μM and 2 μM DHE, with a fixed reductase concentration (1 μg/mL or 27.6 nM). Excitation and emission wavelengths 470 nm and 605 nm, respectively, and 10 nm excitation and emission slits. **Panel B:** Kinetics of DHE oxidation by soluble C*b*$_5$R sensitive to SOD (1 U/mL), in the presence of increasing Cyt *c* concentrations. DHE oxidation was measured as indicated above, in the presence of the Cyt *c* concentrations listed in the figure. The traces shown are averages of experimental triplicates. **Panel C**: Representative traces for the kinetics of Cyt *c* reduction by soluble (black line) and membrane C*b*$_5$R (grey line) with Cyt *c* (3.75 μM), in the absence (continuous lines) and presence (dashed lines) of SOD 1 U/mL. Cyt *c* reduction was measured at 550 nm at 37 °C in the following assay medium (pH 7.0): potassium phosphate 20 mM, DTPA 0.1 mM, Cyt *c* 3.75 μM and NADH 100 μM, with soluble or membrane C*b*$_5$R (0.1 μg/mL). **Panel D**: The $O_2^{\cdot-}$ production rate by soluble (filled squares) and membrane (open squares) C*b*$_5$R dependence upon Cyt *c* is shown. The DHE oxidation rate was measured as indicated in the Panel **A**, with a fixed C*b*$_5$R (1 μg/mL or 27.6 nM)) and DHE concentration (2 μM) in the assay medium. **Panel E**: The $O_2^{\cdot-}$ production by soluble (filled squares) and membrane (open squares) C*b*$_5$R isoforms dependence upon DHE concentration is shown. The DHE oxidation rate was measured as indicated in the Panel A, with a fixed C*b*$_5$R concentrations(1 μg/mL or 27.6 nM) and Cyt *c* (2.5 μM). **Panel F**: Soluble (filled squares) and membrane C*b*$_5$R (open squares) flavin autofluorescence dependence upon Cyt *c* concentration. Cyt *c* elicits a large increase of C*b*$_5$R-flavin autofluorescence that allows measuring C*b*$_5$R: Cyt *c* complex formation by fluorescence. Y-axis: molar fraction of C*b*$_5$R saturated with Cyt *c*, which has been calculated as follows: $\Delta F/\Delta F_{max} = (F\text{-}F_0)/(F_{max}\text{-}F_0)$, where F is the fluorescence intensity at each Cyt *c* concentration, and F_0 and F_{max} are the fluorescence intensity in the absence and saturating concentrations of Cyt *c*, respectively. Fluorescence measurements were performed at 37 °C in the following buffered solution (pH 7.0): 20 mM potassium phosphate, 1 mM EDTA, and 2 μM C*b*$_5$R. Excitation and emission wavelengths 470 nm and 520 nm, respectively, with excitation and emission slits of 10 nm. The averages (± standard errors) of triplicate experiments are shown. Solid and dashed lines are the best non-linear squares fit to the one-binding site equation $(F\text{-}F_0)/(F_T\text{-}F_0) = [\text{Cyt } c]/(K_d + [\text{Cyt } c])$, and yielded values of $R^2 = 0.99$ and 0.98, respectively, for soluble (black line) and membrane (grey line) C*b*$_5$R isoforms.

Table 1
$O_2^{\cdot-}$ production by human C*b*$_5$R.

	Soluble C*b*$_5$R (μmoles/min /mg protein)	Membrane C*b*$_5$R (μmoles/min /mg protein)
NADH oxidase	0.27 ± 0.02	0.15 ± 0.02
O_2 consumption	0.54 ± 0.02	0.33 ± 0.04
$O_2^{\cdot-}$ production (SOD-inhibited NBT reductase)	0.49 ± 0.02	0.26 ± 0.02
Cyt *c* stimulated $O_2^{\cdot-}$ production (DHE)	4.1 ± 0.2[a]	3.5 ± 0.3[a]
Cyt *c* stimulated $O_2^{\cdot-}$ production (DHE)	4.4 ± 0.1[b]	3.8 ± 0.4[b]

[a] Values calculated by fitting the data obtained with DHE to one substrate Michaelis-Menten kinetics.
[b] Values calculated by fitting the data obtained with DHE to two substrates Michaelis-Menten kinetics.

concentrations, we calculated a k_{cat} for $O_2^{\cdot-}$ production by soluble and membrane C*b*$_5$R of 1.45 ± 0.11 and 1.49 ± 0.03 s^{-1} and a K_m for DHE of 0.19 ± 0.01 and 0.25 ± 0.04 μM, respectively (Fig. 4E).

3.3. Measurement of C*b*$_5$R and Cyt c dissociation constant

The results shown above pointed out that Cyt *c* behaves as a redox partner of C*b*$_5$R, opening the possibility to use flavin autofluorescence of C*b*$_5$R to measure the interaction between these two proteins, see e.g. [5].Fig. 4F shows C*b*$_5$R flavin autofluorescence intensity dependence upon Cyt *c* concentration, yielding a large increase of the fluorescence intensity, i.e. between 60 % and 300 % for soluble C*b*$_5$R and for membrane C*b*$_5$R, at saturating concentration of Cyt *c* (5 μM). These results revealed that Cyt *c* interaction with C*b*$_5$R can be appropriately monitored by C*b*$_5$R flavin autofluorescence. The data can be fit to a hyperbolic curve as indicated in the Material and Methods section, yielding a dissociation constant of the Cyt *c*/C*b*$_5$R complex of 0.40 ± 0.05 and 0.38 ± 0.02 μM for soluble and membrane C*b*$_5$R, respectively. Scatchard plot analysis (Supp. Fig. S3) is consistent with the binding of one Cyt *c* molecule per C*b*$_5$R molecule for soluble and membrane isoforms.

4. Discussion

A scheme or the reactions described in this manuscript is shown in Supp. Fig. S4. Our data demonstrate that Cb_5R can use O_2 as an electron acceptor using NADH as substrate. Although the use of DHE for measurement of $O_2^{\cdot-}$ has been stated to be useful for qualitative purposes in biological systems [19], we achieved to quantify $O_2^{\cdot-}$ production by purified Cb_5R with DHE, using proper controls (i.e. calibrating the signal with XA/XO in the presence of a large amount of catalase that avoid E^+ formation when H_2O_2 is also produced) as shown in other reports [10,11,20]. Stoichiometric ratios between NADH and O_2 consumption indicated that Cb_5R uses one NADH molecule to reduce two O_2 molecules. Moreover, the values obtained for $O_2^{\cdot-}$ production correlated with O_2 consumption, indicating that the O_2 consumption is mainly due to $O_2^{\cdot-}$ production (Table 1). With the use of an anti-Cb_5R antibody, we confirmed that Cb_5R was responsible of the Cyt *c* (Fe^{3+}) stimulated production by SPMV, since 90 % of the $O_2^{\cdot-}$ production was blocked by addition of specific antibodies against Cb_5R, added to the assay. As cytochrome P450s also display NAD(P)H-dependent production of $O_2^{\cdot-}$ [21] and some cytochrome P450 isoforms are associated the plasma membrane [22], it is likely that cytochrome P450s account for most of the Cb_5R-independent $O_2^{\cdot-}$ production [22,23], although we cannot discard other $O_2^{\cdot-}$ sources. Our results also show that Cyt *c* binds to purified Cb_5R isoforms with dissociation constants similar to the K_m values for the Cyt *c* stimulated $O_2^{\cdot-}$ production by Cb_5R isoforms and close to the K_m value obtained from the NADH-dependent production of $O_2^{\cdot-}$ by SPMV.

In the context of apoptosis, the function of Cyt *c* reduction by Cb_5R can be seen as part of the cellular defense system, because this protein shows a widespread subcellular membrane localization, namely, endoplasmic reticulum, outer mitochondrial membrane and plasma membrane [24]. Cyt *c* reduction blocks apoptosis since its role in this type of cell death has been mainly attributed to the oxidized form [25–27]. For this reason, systems with ability to reduce Cyt *c* have an intrinsic anti-apoptotic function. Noteworthy, the payback for this reduction exerted by Cb_5R is the formation of $O_2^{\cdot-}$, a radical also described to be formed in mitochondria upon Cyt *c* release [28].

Acknowledgments

This work was supported by the Unidade de Ciências Biomoleculares Aplicadas-UCIBIO, which is financed by national funds from FCT/MEC (UID/Multi/04378/2013) and co-financed by the ERDF under the PT2020 Partnership Agreement (POCI-01–0145-FEDER-007728). Experimental work was also partially supported by funding from Grant BFU2014-53641-P of the Spanish Ministerio de Economía y Competitividad and Ayuda a Grupos de la Junta de Extremadura (GR15139 to Group BBB008) co-financed by the European Funds for Structural Development (FEDER). AKSA and SF thank FCT/MCTES for the post-doctoral and pre-doctoral fellowship grants (SFRH/BPD/100069/2014 and SFRH/BD/84543/2012, respectively), which are financed by national funds and co-financed by FSE. We would like to thank Susana Ramos for her initial assistance in the preparation of the membrane isoform of Cb_5R.

Appendix A. Supporting information

Supplementary data associated with this article can be found in the online version at http://dx.doi.org/10.1016/j.redox.2017.11.021.

References

[1] A.K. Samhan-Arias, M.A. Garcia-Bereguiain, F.J. Martin-Romero, C. Gutierrez-Merino, Clustering of plasma membrane-bound cytochrome b5 reductase within 'lipid raft' microdomains of the neuronal plasma membrane, Mol. Cell. Neurosci. 40 (2009) 14–26.
[2] A.K. Samhan-Arias, D. Marques-da-Silva, N. Yanamala, C. Gutierrez-Merino, Stimulation and clustering of cytochrome b5 reductase in caveolin-rich lipid microdomains is an early event in oxidative stress-mediated apoptosis of cerebellar granule neurons, J. Proteom. 75 (2012) 2934–2949.
[3] A.K. Samhan-Arias, F.J. Martin-Romero, C. Gutierrez-Merino, Kaempferol blocks oxidative stress in cerebellar granule cells and reveals a key role for reactive oxygen species production at the plasma membrane in the commitment to apoptosis, Free. Radic. Biol. Med. 37 (2004) 48–61.
[4] A.K. Samhan-Arias, C. Gutierrez-Merino, Purified NADH-cytochrome b5 reductase is a novel superoxide anion source inhibited by apocynin: sensitivity to nitric oxide and peroxynitrite, Free. Radic. Biol. Med. 73 (2014) 174–189.
[5] A.K. Samhan Arias, R.M. Almeida, S. Ramos, C.M. Cordas, I. Moura, C. Gutierrez-Merino, J.J.G. Moura, Topography of human cytochrome b5/cytochrome b5 reductase interacting domain and redox alterations upon complex formation, BBA Bioenerg. 1859 (2017) 78–87.
[6] A.K. Samhan-Arias, R.O. Duarte, F.J. Martin-Romero, J.J. Moura, C. Gutierrez-Merino, Reduction of ascorbate free radical by the plasma membrane of synaptic terminals from rat brain, Arch. Biochem. Biophys. 469 (2008) 243–254.
[7] A.K. Samhan-Arias, M.A. Garcia-Bereguiain, C. Gutierrez-Merino, Hydrogen sulfide is a reversible inhibitor of the NADH oxidase activity of synaptic plasma membranes, Biochem. Biophys. Res. Commun. 388 (2009) 718–722.
[8] B.H.J. Bielski, G.G. Shiue, S. Bajuk, Reduction of nitro blue tetrazolium by CO_2- and O2- radicals, J. Phys. Chem. 84 (1980) 830–833.
[9] T.V. Sirota, Use of nitro blue tetrazolium in the reaction of adrenaline autooxidation for the determination of superoxide dismutase activity, Biochem. Suppl. Ser. B: Biomed. Chem. 6 (2012) 254–260.
[10] J. Zielonka, J. Vasquez-Vivar, B. Kalyanaraman, Detection of 2-hydroxyethidium in cellular systems: a unique marker product of superoxide and hydroethidine, Nat. Protoc. 3 (2008) 8–21.
[11] H. Zhao, S. Kalivendi, H. Zhang, J. Joseph, K. Nithipatikom, J. Vasquez-Vivar, B. Kalyanaraman, Superoxide reacts with hydroethidine but forms a fluorescent product that is distinctly different from ethidium: potential implications in intracellular fluorescence detection of superoxide, Free. Radic. Biol. Med. 34 (2003) 1359–1368.
[12] M. Hayyan, M.A. Hashim, I.M. AlNashef, Superoxide ion: generation and chemical implications, Chem. Rev. 116 (2016) 3029–3085.
[13] C. Costentin, M. Robert, J.M. Saveant, Concerted proton-electron transfers: electrochemical and related approaches, Acc. Chem. Res. 43 (2010) 1019–1029.
[14] D.T. Sawyer, A. Sobkowiak, J.L. Roberts, Electrochemistry for Chemists, 2nd ed., Wiley, New York, 1995.
[15] T. Araki, H. Kitaoka, The mechanism of reaction of ebselen with superoxide in aprotic solvents as examined by cyclic voltammetry and ESR, Chem. Pharm. Bull. 49 (2001) 541–545.
[16] M. Hayyan, F.S. Mjalli, M.A. Hashim, I.M. AlNashef, Generation of superoxide ion in pyridinium, morpholinium, ammonium, and sulfonium-based ionic liquids and the application in the destruction of toxic chlorinated phenols, Ind. Eng. Chem. Res. 51 (2012) 10546–10556.
[17] J.M. McCord, I. Fridovich, The utility of superoxide dismutase in studying free radical reactions. II. The mechanism of the mediation of cytochrome c reduction by a variety of electron carriers, J. Biol. Chem. 245 (1970) 1374–1377.
[18] J.M. McCord, I. Fridovich, The reduction of cytochrome c by milk xanthine oxidase, J. Biol. Chem. 243 (1968) 5753–5760.
[19] B. Kalyanaraman, V. Darley-Usmar, K.J. Davies, P.A. Dennery, H.J. Forman, M.B. Grisham, G.E. Mann, K. Moore, L.J. Roberts 2nd, H. Ischiropoulos, Measuring reactive oxygen and nitrogen species with fluorescent probes: challenges and limitations, Free. Radic. Biol. Med. 52 (2012) 1–6.
[20] J. Chen, S.C. Rogers, M. Kavdia, Analysis of kinetics of dihydroethidium fluorescence with superoxide using xanthine oxidase and hypoxanthine assay, Ann. Biomed. Eng. 41 (2013) 327–337.
[21] J.B. Schenkman, I. Jansson, The many roles of cytochromeb5, Pharmacol. Ther. 97 (2003) 139–152.
[22] M. Seliskar, D. Rozman, Mammalian cytochromes P450—Importance of tissue specificity, Biochim. Biophys. Acta (BBA) – General. Subj. 1770 (2007) 458–466.
[23] F. Rezende, K.-K. Prior, O. Löwe, I. Wittig, V. Strecker, F. Moll, V. Helfinger, F. Schnütgen, N. Kurrle, F. Wempe, M. Walter, S. Zukunft, B. Luck, I. Fleming, N. Weissmann, R.P. Brandes, K. Schröder, Cytochrome P450 enzymes but not NADPH oxidases are the source of the NADPH-dependent lucigenin chemiluminescence in membrane assays, Free Radic. Biol. Med. 102 (2017) 57–66.
[24] A.K. Samhan-Arias, C. López-Sánchez, D. Marques-da-Silva, R. Lagoa, V. Garcia-Lopez, V. García-Martínez, C. Gutierrez-Merino, J. Neurol. Neuromed. 1 (2016) 61–65.
[25] R. Lagoa, A.K. Samhan-Arias, C. Gutierrez-Merino, Correlation between the potency of flavonoids for cytochrome c reduction and inhibition of cardiolipin-induced peroxidase activity, Biofactors 43 (2017) 451–468.
[26] V. Borutaite, G.C. Brown, Mitochondrial regulation of caspase activation by cytochrome oxidase and tetramethylphenylenediamine via cytosolic cytochrome c redox state, J. Biol. Chem. 282 (2007) 31124–31130.
[27] M.B. Hampton, B. Zhivotovsky, A.F. Slater, D.H. Burgess, S. Orrenius, Importance of the redox state of cytochrome c during caspase activation in cytosolic extracts, Biochem. J. 329 (1998) 95–99.
[28] J. Cai, D.P. Jones, Superoxide in apoptosis. Mitochondrial generation triggered by cytochrome c loss, J. Biol. Chem. 273 (1998) 11401–11404.